Evgeniya Kravchenko and Yuri Kovalev
Astro Space Center of Lebedev Physical Institute, Moscow, Russia

DEPOLARIZATION AND FARADAY EFFECTS IN 20 AGN JETS FROM 1.4 TO 15 GHZ

We present wavelength-dependent analysis of fractional polarization in 20 AGN jets covering 1.4 to 15 GHz. Observations were made with the NRAO VLBA. The study probes parsec-scales properties in both core and jet components. It reveals similar wavelength dependence of fractional polarization in these regions. We applied specific effects to explain observational data and found that depolarization and Faraday effects are common in AGN jets.

DE/REPOLARATIONAL EFFECTS

Effects influence on propagation of electromagnetic wave from place of origin to observer (Faraday 1933, Burn 1966, Gardner&Whiteoak 1966, Pacholczyk&Swihart 1967, Sokoloff et al. 1998):

τ<1 regions (jet components)

N	Effect	Properties	m behavior
1	Simple Faraday-thin screen	Ionized media, located behind the region where emission originates. Media is homogeneous and containing regular magnetic field.	$m=m_{max}\cdot e^{2i\chi}$ $\chi_{observed}=\chi_{intrinsic}+RM\cdot\lambda^2$
2	Random magnetic fields	Random isotropic or anisotropic field, which generally can be imposed on regular (large-scale) field	$m=const$
	Internal Faraday depolarization:		
3	Differential Faraday rotation	Emission originates and propagates in uniform or non-uniform magneto-ionic media, containing ordered magnetic field.	$m=m_{max}\cdot\left\vert\frac{\sin(2\lambda^2 RM)}{2\lambda^2 RM}\right\vert$
4	Internal Faraday dispersion	Emission originates and propagates in inform or non-uniform magneto-ionic media, containing turbulent magnetic field. Characteristic of the depolarization is σ_{RM} – the dispersion of the intrinsic RM within telescope beam.	$m=m_{max}\cdot\frac{1-e^{2\sigma_{RM}^2\lambda^4}}{2\sigma_{RM}^2\lambda^4}$
	External Faraday depolarization:		
5	External Faraday dispersion (“beam depolarization”)	External, non-emitting foreground screen, containing turbulent magnetic field.	$m=m_{max}\cdot e^{2\sigma_{RM}^2\lambda^4}$
6	Partially covering screen (Rossetti-Mantovani law)	External, non-emitting foreground screen, containing turbulent magnetic field, covers only part of the source. Characteristic parameter fc – covered fraction of the source.	$m=m_{max}\cdot[f_c e^{2\sigma_{RM}^2\lambda^4}+(1-f_c)]$
7	RM gradient across the screen	Gradients of Faraday rotation measure (ΔRM) across the beam, originating in the external screen.	$m=m_{max}\cdot\left\vert\frac{\sin(2\lambda^2\Delta RM)}{2\lambda^2\Delta RM}\right\vert$
8	Tribble depolarization	External, non-emitting foreground screen, containing turbulent magnetic field. The ratio of the telescope beam size to the size of RM fluctuations leads to polynomial dependence of fractional polarization with wavelength (A is constant and B is polarization spectral index, varying from -4 to -1).	$m=A\cdot\lambda^B$
9	Anomalous depolarization	Presence of helically shaped magnetic field or tangled large-scale field (A, B – parameters, depending on physical properties of the media and field).	$m\sim m_{max}\cdot\frac{\sin(A-B\lambda^2)}{A-B\lambda^2}$

τ≥1 regions (core components)

In the opaque components dependence from optical depth τ arises additionally to all the effects described above. Generally, it is expected (Fukui 1973, Jones&O'Dell 1977) that fractional polarization grows at frequencies higher (τ<1) and lower (τ>>1) then turnover frequency, meanwhile approaches zero around τ~1.

SOURCES

Our sources were observed quasi-simultaneously with the NRAO VLBA at 1.41, 1.66, 2.28, 2.39, 4.61, 5.00, 8.11, 8.43, and 15.36 GHz (Sokolovsky et al. 2011). The targets were subject of RM study (Kravchenko et al. in prep.) and showed median absolute values in jet components of 44 rad/m^2 and 25 to 699 rad/m^2 in core regions at 1.4-15.4 GHz in the observer's rest frame. The corresponding maximum values are 315 and 2996 rad/m^2.

Source name (B1950)	z	Optical class	Most probable effects τ~1	τ<1
0148+274	1.260	QSO	3, 4, 7, 9	1, 2, 3, 4, 5, 7, 8, 9
0341+147	1.556	QSO	1, 2, 8	3, 4, 5, 7, 9
0425+048	0.517	AGN	3, 4, 7, 9	1, 2, 8
0507+179	0.416	AGN	Any	3, 6, 7
0610+260	0.580	QSO	n/a	n/a
0839+187	1.272	QSO	3, 6, 7	3, 4, 7, 9
0952+179	1.478	QSO	3, 4, 7, 9	1, 2, 8
1004+141	2.707	QSO	3, 6, 7	3, 6, 7
1011+250	1.636	QSO	3, 4, 6, 7, 9	3, 4, 6, 7, 9
1049+250	1.300	QSO	3, 4, 6, 7, 9	1, 2, 8
1219+285	0.161	BLL	3, 4, 7, 9	1, 2, 3, 4, 5, 7, 8, 9
1406-076	1.493	QSO	3, 4, 5, 6, 7, 9	3, 4, 5, 6, 7, 9
1458+718	0.904	QSO	3, 4, 5, 7, 9	3, 4, 5, 6, 7, 9
1642+690	0.751	QSO	3, 6, 7	1, 2, 3, 6, 7, 8
1655+077	0.621	QSO	3, 4, 7, 9	3, 6, 7
1803+784	0.680	QSO	1, 2, 8	3, 4, 7, 9 or 1, 2, 8
1830+285	0.594	QSO	3, 4, 7, 9	3, 4, 5, 7, 9
1845+797	0.056	AGN	n/a	n/a
2201+315	0.298	QSO	3, 6, 7	3, 4, 6, 7, 9
2320+506	1.279	QSO	3, 6, 7	1, 2, 8

Redshifts are from Véron-Cetty&Véron 2010, Finke et al. 2008, Afanasiev et al. 2003

MODEL ACCEPTANCE

To select the model, which better describes the data, Bayesian Information Criterion (Schwarz 1978) was used: $BIC = -2\cdot\ln L + k\cdot\ln(n)$, where L – is the maximized value of log-likelihood of the model, k – number of free parameters and n is the sample size.

RESULTS

Results of the fit (most probable models) are given in the figures and in the table for jet and core components. Two of the sources do not show significant polarized flux density at any of the frequencies. We find that depolarization and Faraday effects are common in AGN jets (see also Farnes et al. 2014, Hovatta et al. 2012, O'Sullivan&Gabuzda 2009). Eight sources show similar and other 10 -- different wavelength dependence of fractional polarization for jet and core components.

Almost all effects, except the Burn and wavelength-independent depolarization, are found as possible interpretation of the data. In the majority of the sources the fractional polarization shows different kind of dependence in the two frequency ranges. It is best described at high (4-15 GHz) and low (1-5 GHz) frequency ranges by different laws. We plan to expand our analysis by modeling EVPA versus wavelength dependence to improve statistics comparing the models.

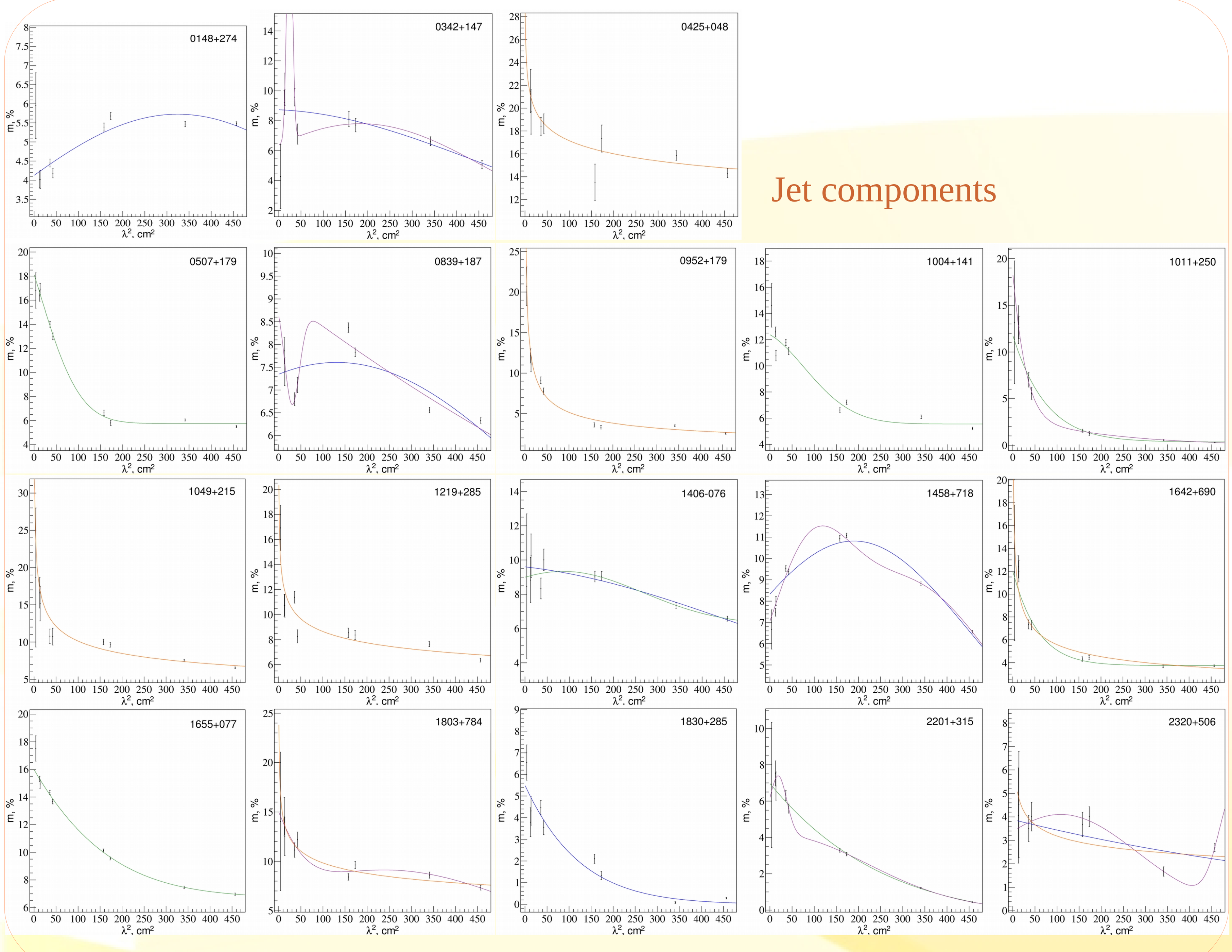

Figures. Fractional polarization vs. wavelength squared (experimental data points with errors) and best fitted models.

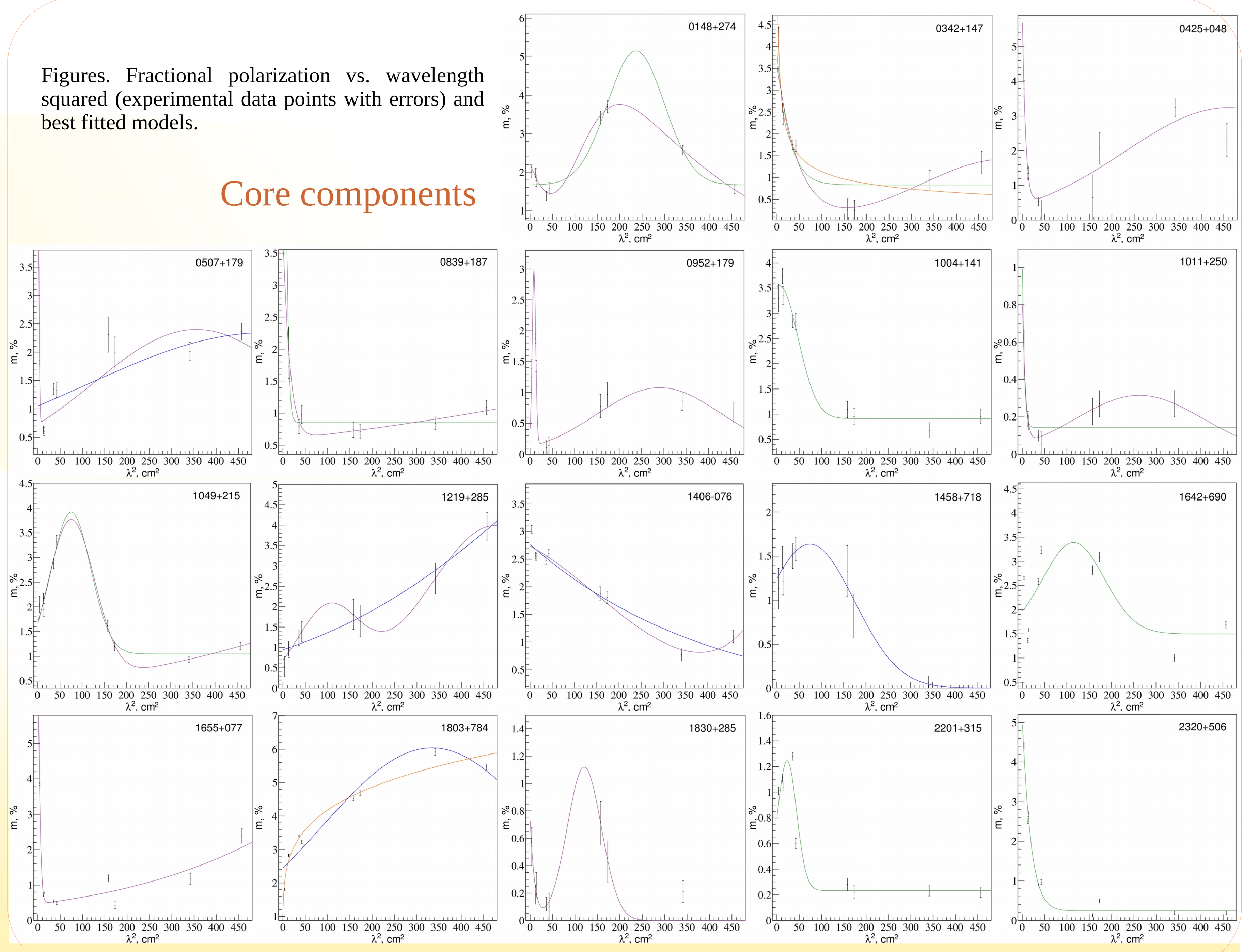

REFERENCES

Afanasiev V. L. et al., 2003, ARep, 47, 458
Faraday M., 1933, in Faraday's Dairy, ed. T. Martin, London: Bell, 264
Burn B. J., 1966, MNRAS, 133, 67
Farnes J.S., Gaenseler B.M. & Carreti E., 2014, ApJS, 212, 15
Finke J.D. et al., 2008, A&A, 477, 513
Fukui Mitsuru, 1973, PASP, 25, 181
Gardner F. F., Whiteoak J. B., 1966, ARA&A, 4, 245
Hovatta T. et al., 2012, AJ, 144, 105
Hovatta T. et al., 2012, AJ, 144, 105
Jones T.W. & O'Dell S.L., 1977, ApJ, 215, 236
O'Sullivan S. P. & Gabuzda D. C., 2009, MNRAS, 393, 429
Pacholczyk A. G. & Swihart T. L., 1967, ApJ, 150
Schwarz G., 1978, Annual Statistics, 6,461
Sokoloff D.D., et al., 1998, MNRAS, 299, 189
Sokolovsky K. V. et al., 2011, A&A, 532, 38
Véron-Cetty M. P. & Véron P., 2010, A&A, 518, A10

“Relativistic Jets: Creation, Dynamics, and Internal Physics”
20-24 April 2015
Krakow, Poland